Interplanetary Magnetic Field Enhancements: Dust or Entangled Flux tubes?

UCLA College | Physical Sciences Earth, Planetary & Space Sciences

Nathan D. Miles[1], Christoper T. Russell[1], Hanying Wei[1], Yingdong Jia[1]

[1]University of California, Los Angeles

AGU

1. Introduction

Observationally, interplanetary magnetic fields enhancements (IFEs) are identified by three distinct properties; a cusp shaped enhancement in the strength of the interplanetary magnetic field, a central current sheet, and a lack of pressure balance between the magnetic field pressure and the thermal pressure of the plasma. In Figure 1, we show the magnetic profile of the typical IFE.

The current formation hypothesis for these structures involves the production of nanoscale dust through collisions between orbital debris associated with asteroids and comets. The neutral dust is ionized by solar radiation and forms a dusty plasma that presents an obstacle to the solar wind flow. Despite a plethora of evidence supporting this hypothesis (Russell (1990), Jones et al. (2003a) Jones et al. (2003b)), a simultaneous detection of dust and an IFE remains elusive.

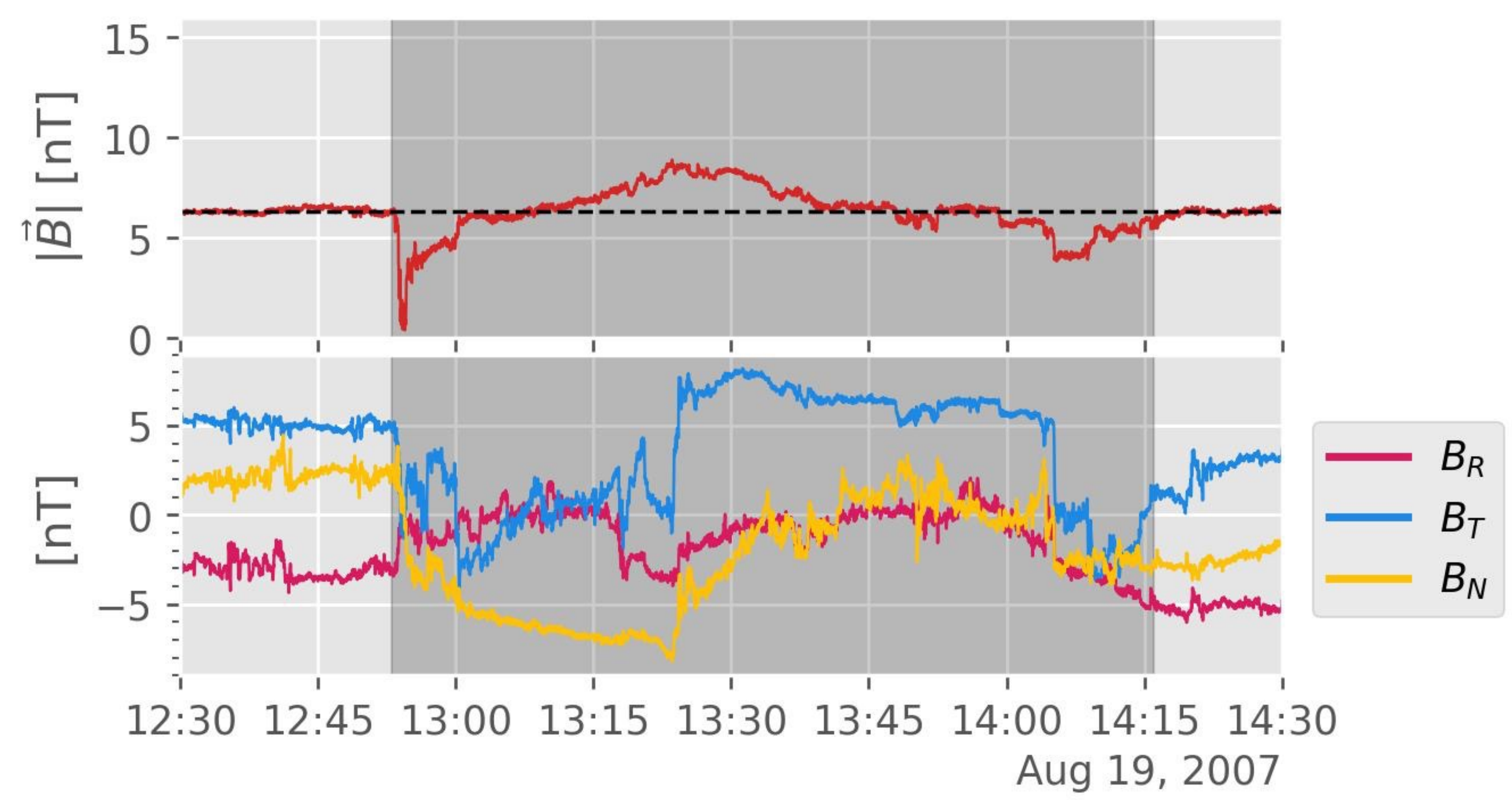

Figure 1: An example IFE detected by the ACE spacecraft. The gray shading marks the region of influence determined by the deviation and return to the background field level denoted by the dashed, black line.

Fargette et al. (2021) reported the identification of magnetic increases with central current sheets (MICCS) in PSP data. Observationally, they look like IFEs but the authors noted that there were no statistically significant increases in the rate of dust impacts as measured by the FIELDS instrument. As a result, the authors have considered them distinct from IFEs. An analysis of the plasma properties suggested that the most likely explanation for these objects is that they are entangled flux tubes like those observed in the dayside magnetopause at Earth (Qi et al. (2020), Fargette et al. (2020)).

Currently, it remains unclear if IFEs and MICCs are indeed truly distinct objects with their own formation mechanisms, or, if they are same object with a single formation mechanism. Here we present the preliminary results of a survey of Solar Orbiter data from June 2020 through February 2022 conducted to address this dilemma.

2. IFE Identification

Peak Finding

- A list of peaks are identified by looking for statistically significant deviations from the nominal background level determined by applying a 1-hour rolling mean filter. In Figure 2, we show an example of the peak finding algorithm.

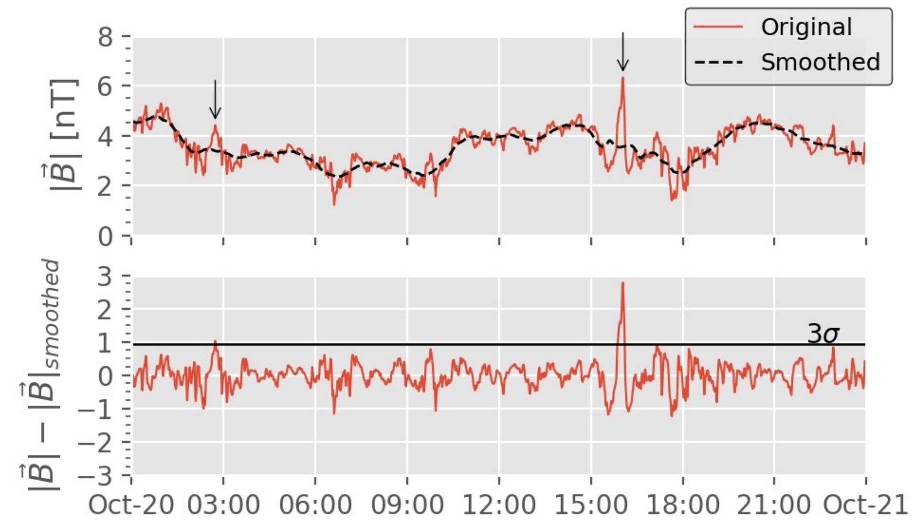

Figure 2: Example peak detection showing two statistically significant deviations

Current Sheet Detection

- For each identified peak, we compute the following,

$$\alpha_i(t) = \left|\frac{\partial \vec{B}_i}{\partial t}\right|.$$

- If $\alpha_i(t)$ attains a maximum within 5 minutes on either side of the peak in the field strength, we mark it as an IFE candidate for follow up with visual inspection before adding to the final list of candidates.

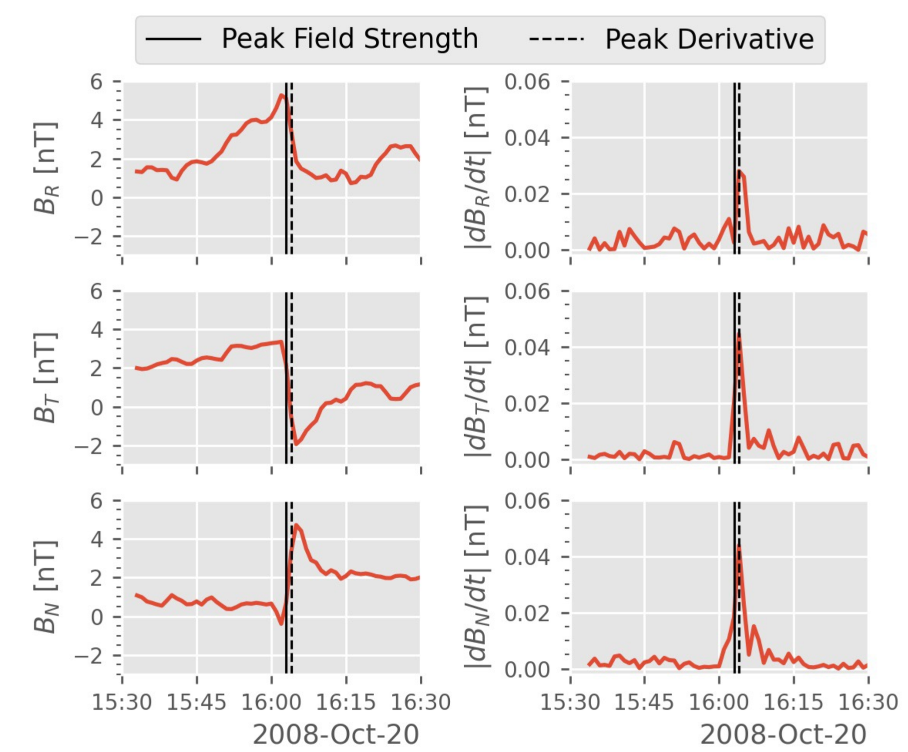

Figure 3: Example current sheet detection for the second peak identified in Figure 2.

3. Statistical Properties

Total IFEs identified: 34

- Mean increase of 37% in $|\vec{B}|$
- Min increase of 7% in $|\vec{B}|$
- Max increase of 93% in $|\vec{B}|$

14/34 had plasma data coverage

- 11 found in slow solar wind $|\vec{u}| < 500\ km\ s^{-1}$
- 1 found in fast solar wind $|\vec{u}| > 600\ km\ s^{-1}$
- 2 are ambiguous $500\ km\ s^{-1} < |\vec{u}| < 600\ km\ s^{-1}$

Event Durations

- Mean duration of 58.1 minutes
- Min duration of 13.5 minutes
- Max duration of 521.7 minutes

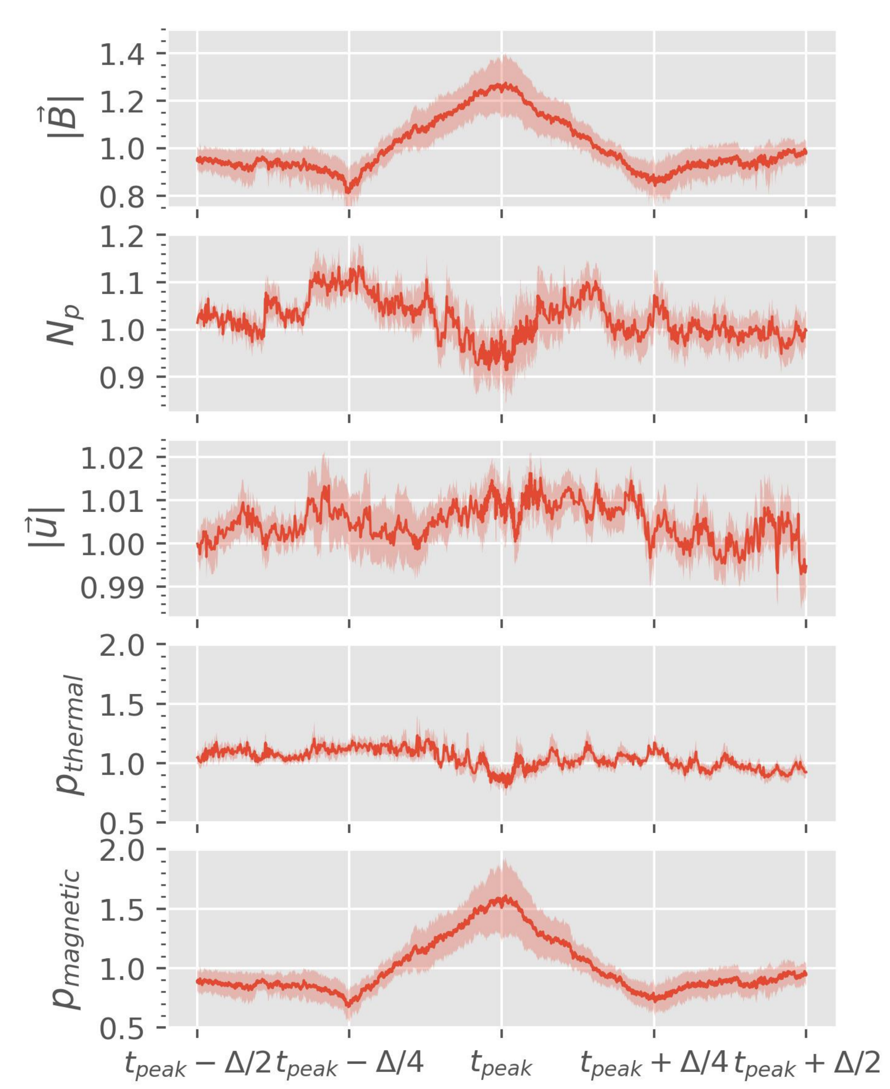

Figure 4: Superposed epoch analysis of all IFEs identified in Solar Orbiter data.

4. August 20th, 2020 IFE

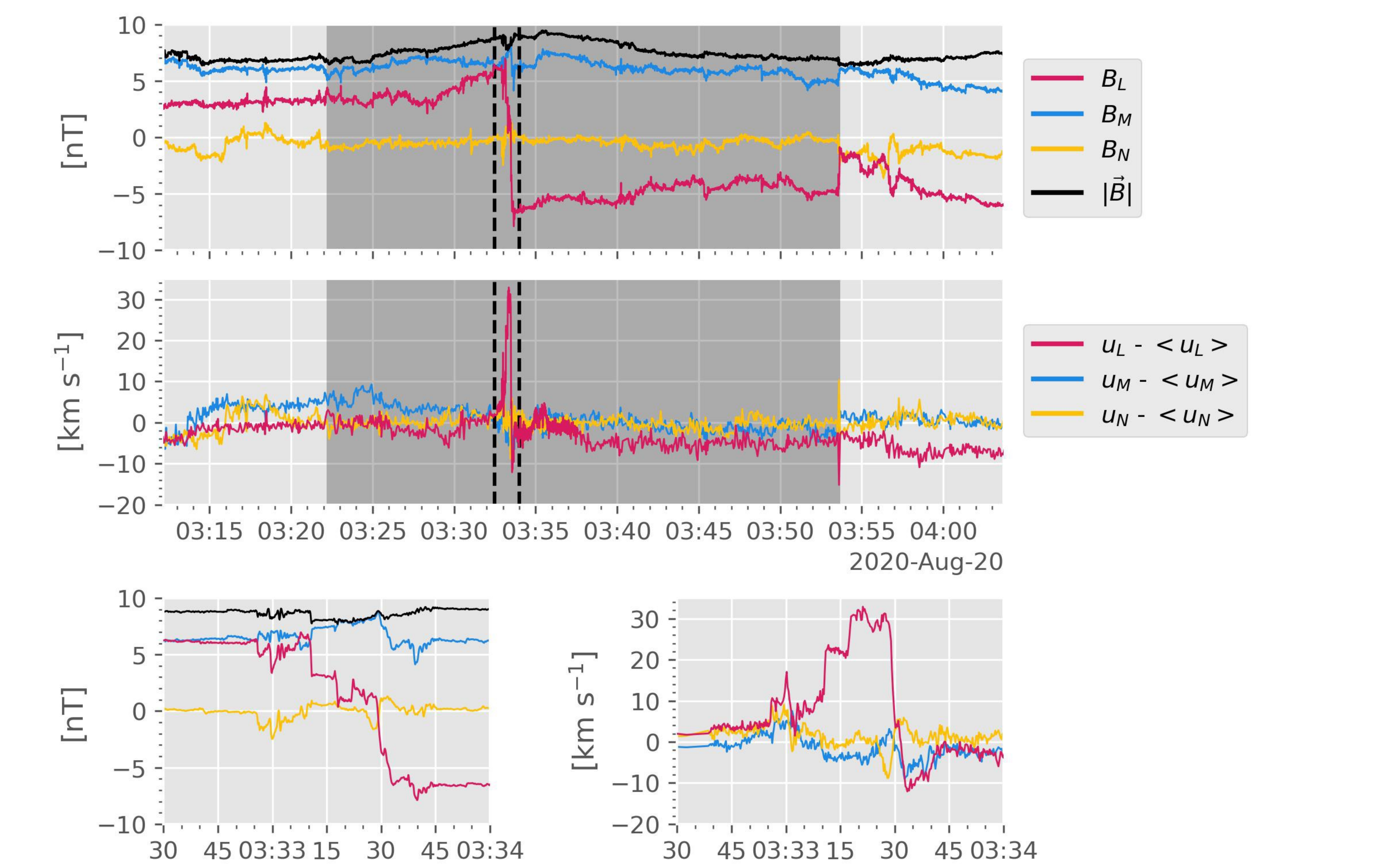

Figure 5: IFE candidate exhibiting reconnection signatures at the central sheet. The top panel shows the magnetic field in LMN coordinates derived using MVAB. Grey shading marks the IFEs region of influence. The next panel shows the components velocity of solar-wind protons, in the same coordinate system, after subtracting off the average value. The bottom left panel shows the magnetic field components during the time interval marked by the vertical dashed lines in the top panel. The bottom right panel shows the velocity component during the same time period.

5. Discussion

On average, $|\vec{B}|$ increased by ~37% and the accompanying enhancement in the magnetic pressure was not compensated by the thermal pressure of the solar-wind plasma (Figure 4). Next, unlike Fargette et al. (2021), we identified an enhancement in the fast solar wind and while this is not the first detection (see Russell et al. (2010)) the disparity between detections in the fast vs slow solar wind is evident. In Figure 5, we show an IFE with a central current sheet showing clear signs of antiparallel magnetic reconnection. At the current sheet, the magnetic field strength drops as energy is converted from magnetic energy to thermal energy. Next, the correlation between B_L and u_L changed across the current sheet going from anti-correlated to correlated as expected for a spacecraft traversing the diffusion region of a magnetic reconnection site. Presently, the identified signatures are still consistent with both hypotheses and require more work to differentiate. For example, applying the GS reconstruction technique to known IFEs to search for presence of multiple flux tubes to test the entangled flux tube hypothesis.

References

- Fargette, N et al. (2020). *Geophysical Research Letters*, *47*(6). https://doi.org/10.1029/2019GL086726
- Fargette, N. et al. (2021). *Astronomy and Astrophysics*, *650*, 1–12. https://doi.org/10.1051/0004-6361/202039191
- Jones, G. H et al. (2003a). *Icarus*, *166*(2), 297–310. https://doi.org/10.1016/j.icarus.2003.09.007
- Jones, G. H., et al. (2003b). *The Astrophysical Journal*, *597*(1), L61–L64. https://doi.org/10.1086/379750
- Qi, Y. et al. (2020) *Geophysical Research Letters*, *47*(23). https://doi.org/10.1029/2020GL090314
- Russell, C. T. (1990). *Advances in Space Research*, *10*(3–4), 159–162. https://doi.org/10.1016/0273-1177(90)90343-X
- Russell, C. T et al. (2010). *Geophysical Research Letters*, *37*(7), n/a-n/a. https://doi.org/10.1029/2010GL042618